ISSN: 2252-8814, DOI: 10.11591/ijaas.v14.i2.pp439-453

Deep learning approach for monkeypox virus prediction: leveraging DensetNet-121 and image data

Kishor Kumar Reddy Chinthala¹, Vijaya Sindhoori Kaza¹, Pilly Ashritha¹, Mohammed Shuaib², Shadab Alam², Mohammad Fakhreldin²

¹Department of Computer Science and Engineering, Stanley College of Engineering and Technology for Women, Hyderabad, India
²Department of Computer Science, College of Engineering and Computer Science, Jazan University, Jazan, Saudi Arabia

Article Info

Article history:

Received Feb 16, 2024 Revised Feb 1, 2025 Accepted Apr 23, 2025

Keywords:

Convolutional neural networks DenseNet-121 Monkeypox Mpox Smallpox Virus prediction

ABSTRACT

The Mpox virus, sometimes referred to as monkeypox, causes flu-like symptoms and rashes. The variola virus, which causes smallpox, is linked to the virus that causes monkeypox. Smallpox symptoms are more severe than those of Mpox, and the illness is rarely deadly. There is no connection between Mpox and chickenpox. The variola virus of smallpox and the vaccinia virus being used in the smallpox vaccine both belong to the Orthopoxvirus genus, which also includes the uncommon viral disease known as monkeypox. This study aims to increase the effectiveness of monkeypox virus (MPV) identification by utilizing global historical records. This study examines several approaches and determines which produces the best results for the input data. Performance metrics have been used to compare the efficiency to current models. The underlying patterns and correlations in the data are then taught to Dense-Net-121 through the use of the training set. The remarkable results are as follows: accuracy at 96.12%, precision at 93.2%, recall at 90%, F1-score at 91%, the area under the curvereceiver operating characteristic (AUC-ROC) at 94.5%, and specificity at 94%, outperforming the existing methods.

This is an open access article under the CC BY-SA license.



439

Corresponding Author:

Mohammed Shuaib

Department of Computer Science, College of Engineering and Computer Science, Jazan University Al Maarefah Rd, Jazan Saudi Arabia

Email: talkshuaib@gmail.com

1. INTRODUCTION

Monkeypox, while typically milder than smallpox, presents symptoms that closely resemble those of its more infamous counterpart. Fever, headaches, muscle aches, and an overall feeling of unwellness are early indicators accompanied by rashes, which typically start from the face and go to other body parts [1]. Since monkeypox is a zoonotic illness, people can contract it from animals [2], [3]. It is known that the main animal reservoirs for monkeypox are rodents [4]. Direct contact with these animals, their bodily fluids, or contaminated objects can expose humans to the virus. Although human cases of monkeypox are rare, the disease poses a significant concern due to its potential for person-to-person transmission, like smallpox [5]. Monkeypox manifests in various dermatological symptoms such as pores on the skin as shown in Figure 1, over-hair growth as shown in Figure 2, burning pores as shown in Figure 3, and skin bulges as shown in Figure 4. The virus poses a global health concern, as illustrated by its spread to non-endemic countries till 15 Jan 2025. Table 1 provides a detailed account of the cases and deaths reported in several countries from Jan 2024 to Jan 2025, which have been collected as per the country's records. Notably, the Democratic Republic of the Congo reported the highest number of cases (9,247) and deaths (43). In contrast, Table 2 provides an overview and comparison of other countries, such as Cameroon and the Central African Republic, which had

440 ☐ ISSN: 2252-8814

significantly fewer cases and deaths, with Cameroon reporting 9 cases and 2 deaths and the Central African Republic reporting 85 cases and 2 deaths. Table 2 also highlights the cases and deaths in countries such as Australia, the United States, the United Kingdom, Belgium, Portugal, Canada, Sweden, Spain, and the Netherlands, indicating the virus's broad geographical reach and the necessity for effective monitoring and control measures [6].



Figure 1. Pores on skin

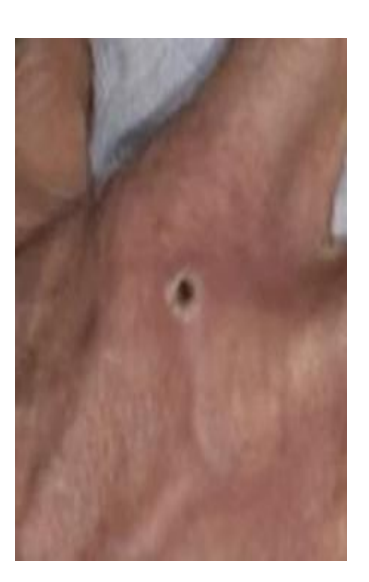


Figure 3. Burning pores



Figure 2. Over hair growth



Figure 4. Skin bulges

Table 1. Representation of Mpox cases and deaths over the country between Jan 2024 to Jan 2025

Country	Cases	Deaths
Australia	1,352	0
Netherlands	125	0
Canada	365	0
Belgium	45	0
Spain	691	0
Portugal	65	1
United Kingdom	271	0
Sweden	38	0
United States of America	4,259	11
Total	7,211	12

Table 2. Statistics about monkeypox virus (MPV) in non-endemic countries between Jan 2024 to Jan 2025

Country	Cases	Deaths
Cameroon	9	2
Central African Republic	85	2
Nigeria	167	0

Diagnosing monkeypox requires a nuanced approach, as various techniques offer advantages and limitations. Virus cultures, explored by Li et al. [7] can detect antibodies in patient serum, but their effectiveness is limited during early stages and may cross-react with related viruses. Similarly, multiplex detection methods employed by Vazquez et al. [8] efficiently identify known viral sequences but might miss novel strains entirely. While virus isolation, demonstrated by Haller et al. [9] as the gold standard, offers definitive proof of infection, it's a time-consuming process requiring high biocontainment facilities, hindering its wider application. Loop-mediated isothermal amplification (LAMP) provides rapid amplification, but sensitivity variations and potential false positives raise concerns [10]. Likewise, ensemble classifiers with mass analysis offer a specific viral protein identification but require specialized equipment and expertise, limiting accessibility [11]. Microarray analysis, another multiplex detection technique used by Sheeja et al. [12], shares limitations with its multiplex counterparts, potentially missing novel strains. Immunofluorescence assay (IFA) offers rapid and accurate results but relies on skilled technicians and specific reagents, posing logistical challenges [13]. Enzyme-linked immunosorbent assay (ELISA) detects antibodies or antigens, but sensitivity limitations hinder its definitive diagnosis [14]. Deep learning (DL) methods, explored by Jaradat et al. [15] offer specific protein detection but require well-characterized antibodies, creating a dependency on existing knowledge. Similarly, artificial neural networks (ANN) and convolutional neural networks (CNN) investigated by Priyadarshini et al. [16] demonstrate high sensitivity but are prone to contamination, requiring careful implementation. Polymerase chain reaction (PCR), highlighted by Azar et al. [17] remains the preferred method due to its high sensitivity and specificity despite the need for specialized equipment and trained personnel. Ultimately, the choice of diagnostic method depends on factors like test availability, resource constraints, and the urgency of results.

The DenseNet-121 model is particularly well-suited for the early, accurate, and reliable identification of monkeypox cases [18]. Its high sensitivity and specificity make it an invaluable tool in medical diagnostics, potentially aiding in the rapid containment and management of monkeypox outbreaks [19], [20]. The model can be extended to other similar infectious diseases with appropriate retraining, thereby broadening its applicability in the field of medical image analysis [21], [22].

While monkeypox cases in humans are considered rare, the virus poses a global health concern because it can transmit from human to human, akin to smallpox [23]. Despite these concerns, gaps in previous research remain significant, particularly in terms of rapid and accurate diagnostics during outbreaks. Previous studies have focused on characterizing the virus and identifying its transmission routes. Still, few have addressed the need for effective, scalable diagnostic methods that can be rapidly deployed in the field [14]. Diagnosing monkeypox traditionally involves several approaches, each with advantages and limitations. Methods like virus isolation and serological tests (e.g., ELISA) have been widely used but are often time-consuming and require specialized laboratory conditions. Emerging techniques like DL models for image-based diagnosis show promise, yet their full potential remains unexplored in the context of monkeypox. No comprehensive study has yet integrated advanced DL methods for rapid, field-deployable diagnostics, which is crucial for timely intervention in outbreak scenarios. Thus, this paper aims to fill these gaps by proposing a novel diagnostic approach utilizing DenseNet-121, a DL model designed for early and correct detection of Mpox through the skin lesion dataset. This paper not only addresses the limitations of traditional diagnostic techniques but also presents a scalable, robust solution that can enhance global efforts in monitoring and controlling monkeypox outbreaks. These are the main contributions of this paper:

- i) Application of DenseNet-121 to the Monkeypox Skin Lesion Dataset (MSLD), the largest and most diverse open dataset available.
- ii) Demonstrating the model's generalization capabilities by testing it on images unrelated to monkeypox.
- iii) Conducting a comprehensive comparison with existing diagnostic models, underscoring the superior performance of DenseNet-121 in terms of accuracy and efficiency.
- iv) The employed DenseNet-121 architecture is characterized by compressed connectivity, dense blocks, growth rate, bottleneck layers, and connectivity to enhance feature extraction and classification accuracy.

The basic architecture of this article is as follows: section 2 describes the techniques, merits, and demerits of relevant work in detail, highlighting the importance of this research and the novelty of the work. Section 3 dives into the details of the proposed architecture and offers a thorough analysis of the databases and the methodology used to build this research work. Section 4 analyses the results to verify the

effectiveness of the architecture and provides a detailed investigation of the performance of the proposed model. The conclusion and further discussion are provided in section 5, which addresses the future directions.

2. RELEVANT WORK

Li et al. [7] intends to meet the growing need for Mpox virus research and diagnostic diagnostics. A zoonotic virus that infects humans and causes a disease akin to smallpox is the Mpox virus, commonly known as the MPV. Li et al. [7] carried out stability tests for the idea in order to evaluate MPXV's activity and viability in several scenarios. One important discovery is that, when held at 37 °C and 20-22 °C, the MPXV titer could maintain more than 86.86% activity for up to 35 days. The paper introduced by Vazquez et al. [8] investigated the genetic composition and evolutionary dynamics of the MPXV during an epidemic in Paraguay. The selection of these specimens was predicated on their satisfactory DNA content, guaranteeing a minimum of 2 ng/µL of DNA. This is done to ensure that the sequencing process produces high-quality genetic data, which is necessary for accurate analysis. Haller et al. [9] proposed that research suggests that the success of a viral infection depends significantly on the virus's capability to manipulate the host's immune response effectively. In her hypothesis, Haller et al. [9] highlights the importance of the virus's ability to interact with the host's immune system in determining the extent of infection and its virulence. According to Haller et al. [9], the evolution of poxviruses, a family of viruses that comprise variola virus and vaccinia virus involves a complex interplay of genetic changes. The usage of LAMP to detect MPV illustrated a sunburst plot of AI research employing Mpox data [10], wherein long short-term memory (LSTM) neural networks were utilized to screen and evaluate a variety of machine learning (ML) and DL methods for diagnosing Mpox with an accuracy of 81.3%.

Rabie and Saleh [11] proposed a new diagnostic strategy for monkeypox, offering the binary tikitaka algorithm (BTTA) feature selection scheme as an efficient method; layered k-nearest neighbors (LKNN), statistical naïve Bayes (SNB), and deep learning classifier (DLC) are the three new base classifiers whose evidence is combined to create a new EC approach by offering a novel voting method known as flux vector splitting (FVS) for combining the choices made by the utilized basic classifiers. To verify the effectiveness and appropriateness of the suggested diagnosing approach, independent assessments were carried out using two different datasets with a 79% accuracy rate. Sheeja et al. [12] proposed a significant endeavor in the field of infectious disease research, mainly focusing on monkeypox (Mpox). With the alarming increase in emerging infectious diseases, understanding the trajectory and productivity of research in this area is crucial for effective response strategies and public health interventions. A comprehensive analysis of scientific publications pertaining to the MPV, leveraging bibliometric techniques and visualization tools, the study aims to unearth key insights into the landscape of MPV research, spanning the years 2001 to 2021 [14]. The dataset under scrutiny comprises 501 scientific publications sourced from the Scopus database, representing a substantial corpus of scholarly work dedicated to the study of MPV. Vierbaum et al. [13] proposed a study that examined the first German EQA's quantitative and qualitative data for the identification of MPXV and orthopoxviruse (OPXV) DNA. Three MPXV-positive samples with varying MPX virus loads and one negative sample were included in the survey. An assay-specific analysis was conducted on the threshold cycle (Ct) or other metrics that define the quantification cycle (Cq).

Jaradat et al. [15] proposed a variety of criteria, such as scoring metrics, and optimizer along loss function, that were used to assess the model's performance. Due to the binary nature of the categorization (i.e., monkeypox and non-monkeypox), the binary_crossentropy loss function was selected. The purpose of the study was to enhance DL-based techniques for Mpox identification in order to outperform the current system, which uses the MobileNetV2 algorithm to achieve 94.2% best validation accuracy. Priyadarshini et al. [16] proposed a significant development in the application of cutting-edge techniques to epidemiological research. With the aim of providing a comprehensive understanding of monkeypox outbreaks, the study harnesses the power of ML and time series analysis methodologies. The reported accuracy of 87% achieved by Priyadarshini et al. [16] research in 2023 underscores the effectiveness and reliability of the proposed method. High accuracy rates indicate the robustness of the ML models and time series analysis techniques employed, instilling confidence in the study's findings and predictive capabilities. Azar et al. [17] proposed that the study represents a significant advancement in the domain of clinical image analysis and disease diagnostics. By applying DL techniques, specifically deep neural networks (DNNs), the study aims to develop robust algorithms capable of accurately identifying cases of monkeypox based on medical images. A summary of existing work, highlighting its limitations along with its merits, is provided in Table 3.

The proposed DenseNet-121 model significantly outperforms existing methodologies for MPV prediction by leveraging its compressed connectivity, dense blocks, and bottleneck layers to enhance feature extraction and classification accuracy. Unlike traditional methods such as MPXV cultures and PCR, which

require specialized equipment and are prone to limitations like cross-reactivity and false positives, the DenseNet-121 model offers robust performance even when tested on non-monkeypox images. This model's application to the largest and most diverse open dataset, the MSLD, demonstrates its superior accuracy and generalization capabilities, providing a more reliable and scalable solution for rapid diagnosis compared to prior approaches.

Table 3. Analysis of the existing approaches

References	Methodology proposed	Merits	Demerits
[7]	MPXV cultures	Detects antibodies in patient serum	Limited during early infection, may cross-react with
			related viruses
[8]	MPXV cultures	Multiplex detection of viral genes	Limited to known sequences, may miss novel strains
[9]	Virus Isolation	Definitive proof of infection	It is time-consuming and may require high biocontainment
[10]	LAMP	Rapid and isothermal amplification	Sensitivity may vary, and false positives can occur
[11]	Ensemble classifiers	Identifies viral proteins through mass	Equipment and expertise required
	with mass	analysis	
[12]	Microarray analysis	Multiplex detection of viral genes	Limited to known sequences, may miss novel strains
[13]	ELISA	Detects antibodies or antigens	Limited in terms of sensitivity
[14]	IFA	Rapid results with high accuracy	Requires skilled technicians and specific reagents
[15]	DL-based methods	Detects specific proteins	Requires well-characterized antibodies
[16]	CNN and ANN	Amplifies DNA/RNA at a constant	Sensitive, but may be prone to contamination
		temperature	
[17]	PCR	High sensitivity and specificity	Requires specialized equipment and trained personnel

3. MATERIALS AND METHOD

3.1. Monkeypox skin lesion dataset description

This work leverages a curated dataset comprised of original and augmented images. The initial dataset consisted of 228 images, with a near-balanced distribution: 102 images (45%) in the "monkeypox" class and 126 images (55%) in the "others" class. The "others" class encompasses unrelated conditions, such as measles and chickenpox, serving as essential negative controls for the classification task. To enhance the dataset's robustness and improve classification performance, data augmentation techniques were meticulously applied using MATLAB R2020a. This process strategically introduced controlled variations to the original images, mimicking real-world scenarios encountered during image acquisition. Techniques employed included hue, saturation, contrast, and brightness adjustments, simulating variations in lighting conditions. Additionally, noise injection, scaling, translation, reflection, shear, and rotation were utilized to create realistic image transformations. This data augmentation strategy resulted in a significant expansion of the dataset size. The "monkeypox" class witnessed a substantial increase to 1428 images, representing a 14-fold expansion. Similarly, the "others" class grew to 1,764 images. This significant increase in data volume is expected to improve the model's performance. To ensure statistically robust evaluation and minimize potential bias, a three-fold cross-validation approach was implemented. Here, the original, un-augmented images were strategically divided into training, validation, and test sets in a 70:10:20 ratio. This approach prioritizes patient anonymity (patient autonomy) while minimizing bias toward specific data points notably, the test set is comprised solely of the original images, preserving their unaltered nature. Conversely, only the training and validation sets underwent data augmentation, fostering flexibility and allowing researchers to either apply their own algorithms to the original data in the test set or directly utilize the pre-defined folds for evaluation.

Figure 5 shows histopathology images of MPV infections where Figure 5(a) presents a transmission electron micrograph (TEM) and illustrates a morphologically mature MPV virion. The central electron-dense core, exhibiting an ovoid to brick-shaped morphology, encapsulates the viral genome and associated proteins. The intricate surface structure represents the mature virion's outer envelope, a complex multi-layered membrane essential for host cell attachment, entry, and subsequent infection. The stippled background likely consists of residual cellular components or staining precipitates inherent to TEM sample preparation. This image provides ultrastructural insight into the infectious particle of MPV, highlighting key features relevant to its interaction with host cells during the pathogenesis of monkeypox. Figure 5(b) presents a histopathological section of tissue stained with hematoxylin and eosin (H&E), demonstrating lentiginous melanocytic proliferation. The epidermis, stained pink, exhibits an increased number of melanocytes, particularly at the dermo-epidermal junction. These melanocytes, which produce melanin, appear as darker nuclei against the lighter pink background. The underlying dermis shows a mixed inflammatory infiltrate. This pattern is characteristic of lentiginous melanocytic proliferation, often seen in conditions such as lentigo maligna or certain types of melanomas in situ. The H&E stain highlights cellular morphology and tissue architecture, enabling the assessment of melanocytic density and distribution within the tissue sample.

Figure 5(c) illustrates a low-magnification (10x) view of a H&E-stained section revealing an excised lesion characterized by a distinct lobular architecture. The lesion is composed of multiple rounded or irregular compartments (lobules) separated by connective tissue septa. The cellular composition within these lobules and the staining patterns varies across the sub-images (A-J), indicating potential heterogeneity within or between different samples of such lesions. Figure 5(d) presents immunohistochemical staining for the DNA repair protein XRCC4 across different tissue sections (A-H). The brown staining indicates the presence and localization of XRCC4 protein, while the blue counterstain (likely hematoxylin) visualizes the cell nuclei. The varying patterns and intensity of XRCC4 staining across the sub-images suggest differential expression of this protein in different cell types and tissue compartments.

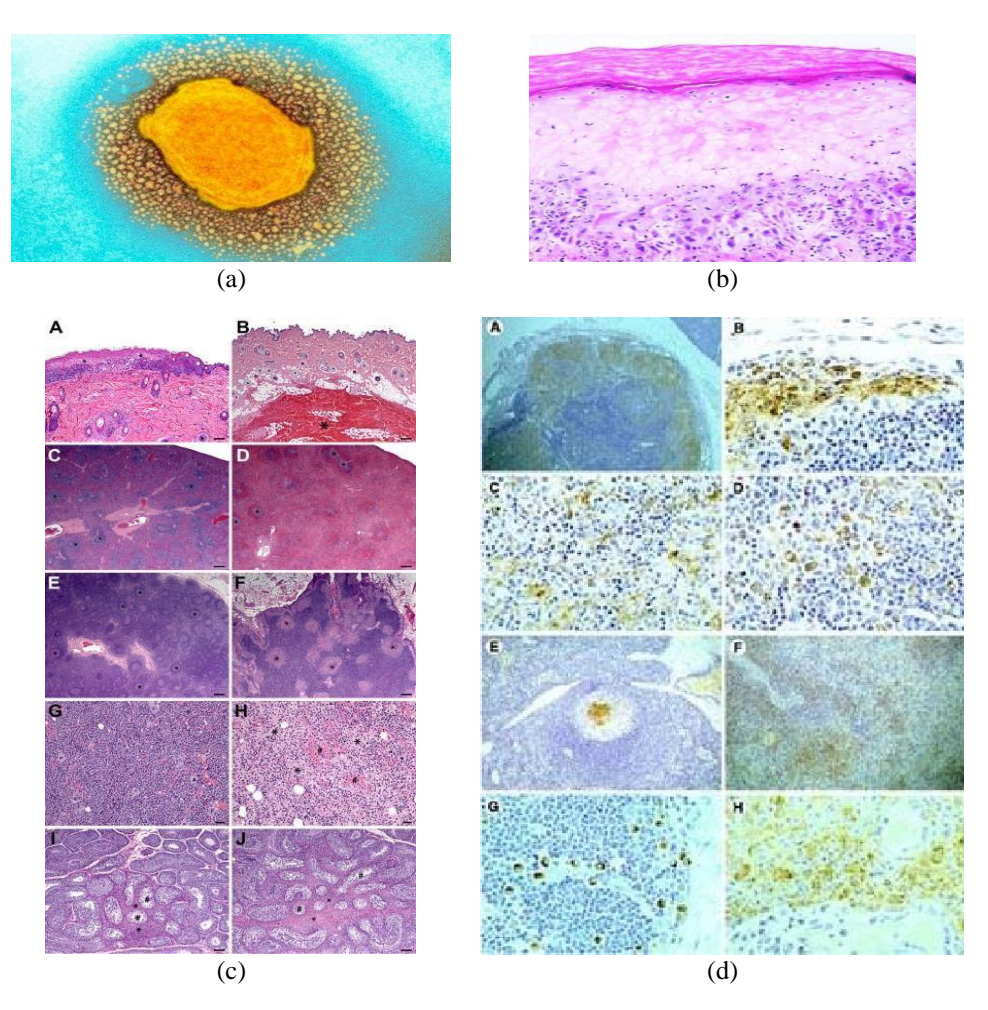


Figure 5. Histopathology images of MPV infections of (a) transmission electron micrograph of a mature monkeypox virion, (b) histopathological analysis of lentiginous melanocytic proliferation with H&E stain, (c) low power histopathology of an excised lesion exhibiting lobular architecture, and (d) immunohistochemical staining for XRCC4 protein in various tissue samples

3.2. Proposed DenseNet-121 model architecture for Monkeypox prediction

The application of DenseNet-121, a CNN architecture, to the identification of the MPV, has transformed the field of medical image analysis. The 'vanishing gradient' problem is addressed by DenseNet-121, which makes sure that data is preserved as the network gets deeper. As seen in Figure 6, every layer is directly connected to every other layer, improving the gradients and information flow throughout the network. Using DenseNet-121 for virus detection requires a few crucial actions. The DenseNet-121 model is one of the models in the DenseNet group designed for picture categorization. Trained initially on Torch*, the models were eventually converted to Caffe* format by the authors. Every DenseNet-121 model was pretrained using the ImageNet database. CNN Layers contain multiple layers, which are explained briefly as follows.

Assume that an N×N square neuron layer is before the convolutional layer. The output of the convolutional layer, when using a m×m filter ω , will be $(N-m+1)\times(N-m+1)$. The pre-nonlinearity input to some unit x_{ij}^l in the layer can be computed by adding the contributions from the cells in the previous layer, weighted by the filter components shown in (1).

$$x_{ij}^{l} = \sum_{a=0}^{m-1} 1 \sum_{b=0}^{m-1} \omega ab y^{l-1} (i+a)(j+b)$$
 (1)

This is merely a convolution, which conv2(x, w, 'valid') in MATLAB expresses. Next, the nonlinearity of the convolutional layer is applied as shown in (2).

$$y_{ij}^l = \sigma(x_{ij}^l) \tag{2}$$

DenseNet-121 consists of dense blocks and transition layers that are depicted in detail in Figure 8. If there are L layers in a dense block, then each layer receives the feature maps from all of the layers that came before it, creating L(L+1)/2 direct connections. This architecture makes better gradient flow and more effective training possible. The dense blocks maintain feature map sizes for concatenation while transition layers down the sample through convolution and pooling processes, as depicted in Figures 7 and 8. The architecture of the proposed model with all three dense blocks is shown in Figure 9.

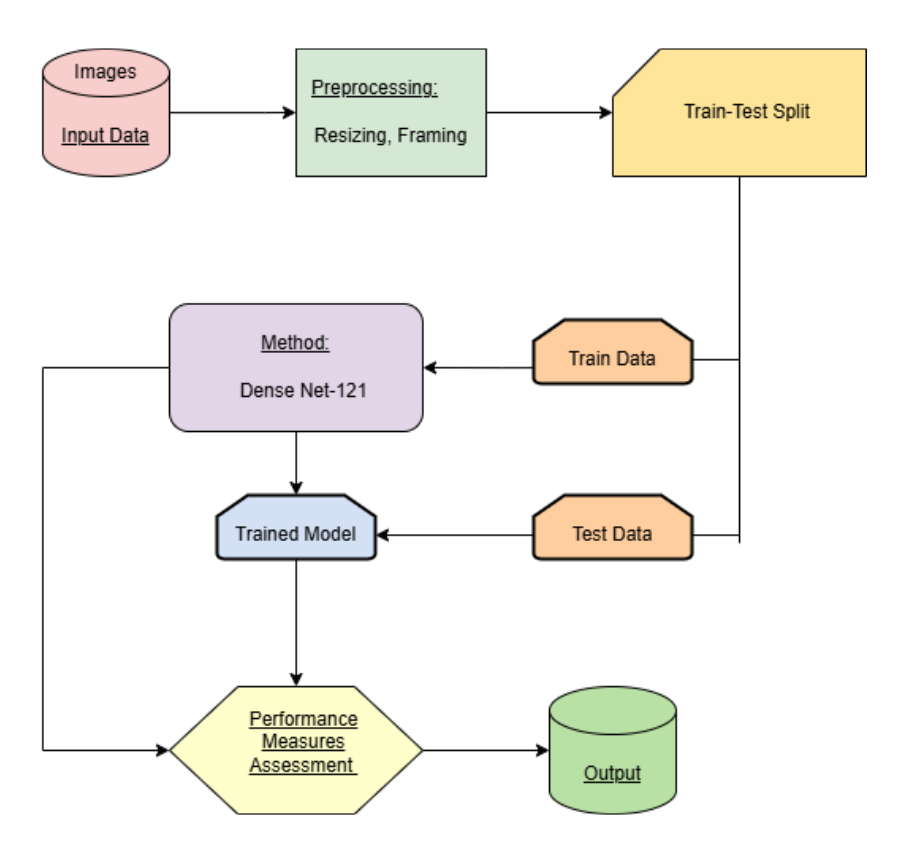


Figure 6. DenseNet-121 architecture for MPV

3.3. Max-pooling layers

The max-pooling layers are fairly simple but do not support self-learning. They only produce a single result, which is the greatest value of a given $k \times k$ rectangle. For instance, because the max function lowers each $k \times k$ block to a single value, if their input layer is an $N \times N$ layer, they will output an $N/k \times N/k$ layer.

3.4. Convolutional layers

Note that the error that we know and must compute for the previous layer is the partial of E with regard to each neuron output $\frac{\partial E}{\partial y_{ij}^L}$. First, let's find the gradient component for each weight using the chain rule.

446 □ ISSN: 2252-8814

Remember that the chain rule requires the contributions of all expressions that contain the variable to be added up. In (3) described as follows,

$$\frac{\partial E}{\partial \omega ab} = \sum_{i=0}^{N-m} \sum_{j=0}^{N-m} \frac{\partial E}{\partial x} \frac{\partial x_{ij}^{l}}{\partial \omega a} = \sum_{i=0}^{N-m} \sum_{j=0}^{N-m} \frac{\partial E}{\partial x} y^{(i+a)(j+b)}$$
(3)

That it resembles a convolution a little bit! The filter ω is applied to the layer in some way, but the result is $\chi_{(i-a)(j-b)}$ rather than $\chi_{(i+a)(j+b)}$. Furthermore, take note of the fact that the aforementioned statement only makes sense for positions that are at least m from the left and top boundaries. We need to add zeros to the top and left edges in order to correct this. If that's the case, this is just an ω convolution that has been flipped in both directions.

Each layer in Figure 7 represents the step-by-step procedure of Dense-Net-121. The 'vanishing gradient' issue, however, appears as the CNN gets deeper or has more layers. This implies that some information may "vanish" or "be lost" as the channel from the input to the output layers widens, which would hinder the network's capacity to train efficiently. DenseNets address this problem by changing the conventional CNN architecture and streamlining the connectivity pattern across layers. The DenseNet design connects each layer to every other layer, hence the phrase "densely connected convolutional networks." Direct connections between "L" levels are of length L(L+1)/2. Three dense blocks make up a deep DenseNet in the picture above. The feature maps within the dense block are all the same size to enable feature concatenation, while the transition layers separating two adjacent blocks perform down sampling (i.e., altering the size of the feature maps) through convolution and pooling procedures.

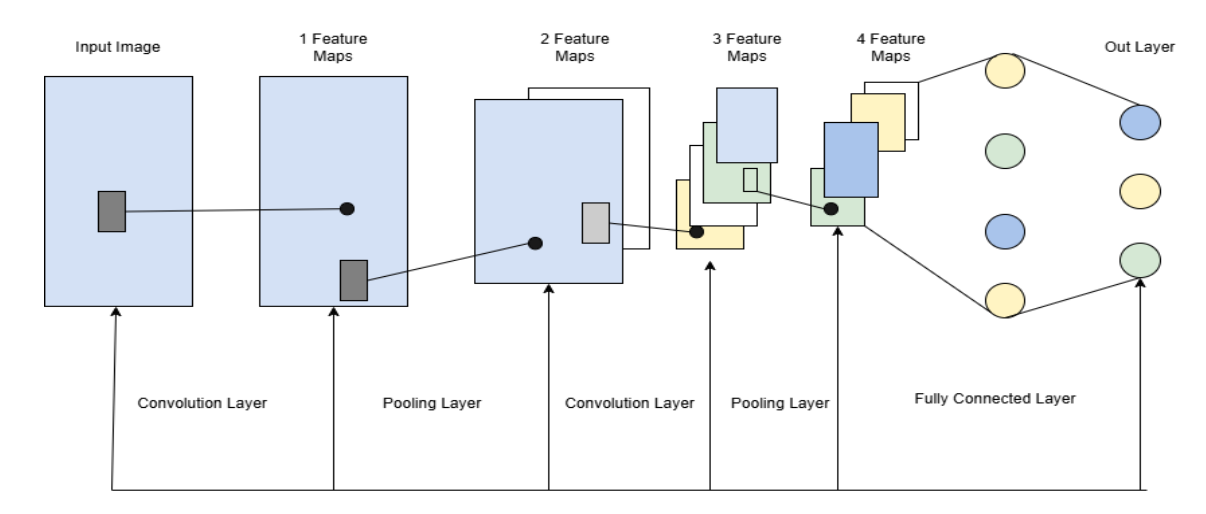


Figure 7. DenseNet-121-layer representation

Layers	Output Size	DenseNet-121	DenseNet-169	DenseNet-201	DenseNet-264							
Convolution	112 × 112	7×7 conv, stride 2										
Pooling	56 × 56		$3 \times 3 \text{ max } \text{ J}$	pool, stride 2								
Dense Block (1)	56 × 56	$\left[\begin{array}{c} 1 \times 1 \text{ conv} \\ 3 \times 3 \text{ conv} \end{array}\right] \times 6$	$\left[\begin{array}{c} 1 \times 1 \text{ conv} \\ 3 \times 3 \text{ conv} \end{array}\right] \times 6$	$\begin{bmatrix} 1 \times 1 \text{ conv} \\ 3 \times 3 \text{ conv} \end{bmatrix} \times 6$	$\left[\begin{array}{c} 1 \times 1 \text{ conv} \\ 3 \times 3 \text{ conv} \end{array}\right] \times 6$							
Transition Layer	56 × 56		1 × 1	conv								
(1)	28 × 28		2 × 2 average	e pool, stride 2								
Dense Block (2)	28 × 28	$\left[\begin{array}{c} 1 \times 1 \text{ conv} \\ 3 \times 3 \text{ conv} \end{array}\right] \times 12$	$\left[\begin{array}{c} 1 \times 1 \text{ conv} \\ 3 \times 3 \text{ conv} \end{array}\right] \times 12$	$\left[\begin{array}{c} 1 \times 1 \text{ conv} \\ 3 \times 3 \text{ conv} \end{array}\right] \times 12$	$\left[\begin{array}{c} 1 \times 1 \text{ conv} \\ 3 \times 3 \text{ conv} \end{array}\right] \times 12$							
Transition Layer	28 × 28		1 × 1	conv								
(2)	14 × 14		2×2 average pool, stride 2									
Dense Block (3)	14 × 14	$\left[\begin{array}{c} 1 \times 1 \text{ conv} \\ 3 \times 3 \text{ conv} \end{array}\right] \times 24$	$\left[\begin{array}{c} 1 \times 1 \text{ conv} \\ 3 \times 3 \text{ conv} \end{array}\right] \times 32$	$\left[\begin{array}{c} 1 \times 1 \text{ conv} \\ 3 \times 3 \text{ conv} \end{array}\right] \times 48$	$\left[\begin{array}{c} 1 \times 1 \text{ conv} \\ 3 \times 3 \text{ conv} \end{array}\right] \times 64$							
Transition Layer	14 × 14	707	1 × 1	conv	*************************************							
(3)	7 × 7		2 × 2 average	e pool, stride 2								
Dense Block (4)	7 × 7	$\left[\begin{array}{c} 1 \times 1 \text{ conv} \\ 3 \times 3 \text{ conv} \end{array}\right] \times 16$	$\left[\begin{array}{c} 1 \times 1 \text{ conv} \\ 3 \times 3 \text{ conv} \end{array}\right] \times 32$	$\left[\begin{array}{c} 1 \times 1 \text{ conv} \\ 3 \times 3 \text{ conv} \end{array}\right] \times 32$	$\left[\begin{array}{c} 1 \times 1 \text{ conv} \\ 3 \times 3 \text{ conv} \end{array}\right] \times 48$							
Classification	1 × 1	VIII.	7 × 7 global	average pool	127							
Layer			1000D fully-connected, softmax									

Figure 8. Layer-to-layer representation of DenseNet-121

Figure 9. The proposed architecture, including the three Dense blocks

The proposed model was further refined on the MSLD, which consists of 3,192 images of monkeypox and different conditions, after being pre-trained using the ImageNet image collection. The model's convolutional layers utilize m×m filters to compute the pre-nonlinearity input to each unit, as described in (1). The nonlinearity is applied as shown in (2), and max-pooling layers reduce the dimensionality of the feature maps by selecting the maximum value in k×k rectangles. The DenseNet-121 architecture was evaluated and compared with other models using various performance measures. The model demonstrated superior accuracy and generalization capabilities, providing a more reliable solution for rapid diagnosis of monkeypox compared to traditional methods such as MPXV cultures, PCR, and other ML techniques, as discussed in Table 1.

An overview of this methodology is described in Algorithm 1. This study uses a clear pathway to train and assess a deep-learning model for classifying images of monkeypox. In order to ensure a balanced portrayal of monkeypox and related disorders, the procedure begins with input data preparation, which involves gathering photos from multiple sources. For better model convergence, these photos are subsequently pre-processed by normalizing their pixel values and shrinking them to a standard size. Data augmentation techniques are used with MATLAB R2020a to enrich the dataset further and improve the generalisability of the model. These methods imitate real-world situations by adding carefully chosen modifications to the pictures. A three-fold cross-validation method is then used to carefully divide the enhanced dataset into training (70%), validation (10%), and test sets (20%). This ensures no data leakage between sets and allows for robust model evaluation with minimized bias.

Algorithm 1. DenseNet-121 for monkeypox detection

- i) Getting the data ready
 - Gather and prepare the dataset.
 - Use approaches for data augmentation.
 - Divide the dataset into sets for testing, validation, and training.
- ii) Initialization of the model
 - Open the DenseNet-121 model that has already been trained.
 - Adjust the last fully connected layers to correspond with the dataset's class count (monkeypox and others).

iii) Training phase

- Set up the training settings (epochs, batch size, and learning rate).
- For every training set batch and every epoch:
- Forward pass: use DenseNet-121 to process input pictures.
- Utilizing the selected loss function, calculate the loss.
- Compute gradients in the backward pass.
- Using an optimization algorithm (like Adam), update the model weights.

iv) Validation phase

- Evaluate the model on the validation set.
- Monitor performance metrics (accuracy, loss) to check for overfitting or underfitting.
- Adjust hyperparameters if necessary.
- v) Testing phase
 - Evaluate the trained model on the test set.
 - Calculate final performance metrics.
- vi) Model deployment
 - Save the trained model.
 - Deploy the model for real-time monkeypox detection.

Next comes model initialization. The DenseNet-121 architecture, pre-trained on the massive ImageNet dataset, is employed as a starting point. The final layers of this pre-trained model are replaced with

448 □ ISSN: 2252-8814

new ones specific to the two-class classification task (monkeypox and others). These new layers are then initialized using appropriate techniques. Hyperparameters such as learning rate, batch size, and the number of training epochs are specified during the training phase. To further direct the training process, an optimizer (like Adam) and a loss function (like cross-entropy loss) are selected. During training, batches of images from the training set are fed into the model, predictions are generated, and the loss between these predictions and true labels is calculated. This loss is then used to update the model's weights through backpropagation, gradually improving its classification accuracy. The validation phase plays a crucial role in preventing overfitting or underfitting. Metrics like accuracy, precision, recall, and F1-score are used to assess the model's performance on the validation set following each training epoch. Based on these metrics, hyperparameters can be adjusted to fine-tune the training process. Lastly, the unseen test set is used to assess the trained model thoroughly. This offers a last evaluation of the model's capacity to generalize and categorize fresh data. The test set can be subjected to error analysis in order to pinpoint specific failure scenarios and guide future model enhancements. For later usage, the trained model is stored in an appropriate format that includes model weights and pre-processing processes. As a result, the model can be implemented in a real-time detection system, where fresh photos can be pre-processed, categorized using the learned model, and possibly utilized for medical diagnosis. To keep the deployed model functional, it is essential to keep an eye on its performance and update it with fresh data.

4. RESULTS AND DISCUSSION

The results section typically provides a detailed description and analysis of the findings obtained from the study. It is crucial as it presents the evidence that supports or refutes the study's hypothesis or research questions. Here's a breakdown of the results for this paper's proposed model accuracy at 96.12%, precision at 93.2%, recall at 90%, F1–score at 91%, AUC-ROC at 94.5%, and specificity at 94%.

In (4) is used to implement many models and compare them in order to analyze accuracy. Generally speaking, one popular assessment criterion for assessing a classification model's performance is accuracy. It shows the percentage of cases (or data points) that were accurately predicted relative to the total number of occurrences or cases in the dataset. When the dataset is well-balanced-that is, when the classes are represented approximately equally-accuracy is extremely helpful. Table 4 shows a comparison between different models for accuracy, which are obtained as follows: The model proposed so-called DenseNet-121 with the highest accuracy of 96.12%, and then ANN at 89.00%, random forest (RF) with different optimizers model with 88%, SVM at 87%, logistic regression (LR) at 85% and decision tree (DT) at 80%.

$$Accuracy = \frac{TP + TN}{TP + TN + FP + FN} \tag{4}$$

According to (5), precision is a performance parameter used in statistics and ML to assess how accurately a model makes positive predictions. In relation to the total number of anticipated positive occurrences, it indicates the proportion of expected positive cases that are real positives. Table 4 shows a comparison between different models for precision, which are obtained as follows: DenseNet-121 with the highest precision of 93.2% and then ANN at 92.00%, RF with 90%, SVM at 89%, LR at 88%, and DT at 82%.

$$Precision = \frac{TP}{TP + FP} \tag{5}$$

Another performance indicator utilized in statistics, especially when dealing with binary classification problems, is recalled. It gauges how well a model can distinguish every positive event from the total number of real positive events in the dataset. Table 4 shows a comparison between different models for recall, which are obtained as follows: DenseNet-121 with the highest recall of 90% and then ANN at 88%, RF with 86%, SVM at 85%, LR at 82%, and DT at 78%. In binary classification, recall is calculated using the formula given in (6),

$$Recall = \frac{Tp}{TP + FN} \tag{6}$$

The F1-score is a performance statistic commonly used in binary classification problems, where there are two classes: positive and negative. Table 4 shows a comparison between different models for F1-score, which are obtained as follows: DenseNet-121 with the highest recall of 91% and then ANN at 90%, RF with 88%, SVM at 87%, LR at 85%, and DT at 80%. The formula for F1-score is given in (7),

$$F1 - score = \frac{2*(precision*recall)}{(precision+recall)}$$
(7)

One approach for assessing the performance of an ML model is the AUC ROC curve. Although there are numerous methods for determining the ROC AUC score, the trapezoidal rule is a commonly used way. This entails creating trapezoids with vertical lines at the false positive rate (FPR) values and horizontal lines at the true positive rate (TPR) values to approximate the area under the ROC curve. Table 4 shows a comparison between different models for AUC ROC, which are obtained as follows: DenseNet-121 with the highest AUC ROC of 94.5% and then ANN at 94%, RF at 93%, SVM at 92%, LR at 91% and DT at 88%. AUC ROC formulation,

$$AUC - ROC = \int_0^1 (TP(FPR)dFPR) dFPR$$
 (8)

Specificity is a measure used in diagnostic testing to assess how well a test correctly identifies individuals without a particular condition or disease. Figure 10 shows a comparison between different models for Specificity, which are obtained as follows: DenseNet-121 with the highest specificity of 94% and then ANN at 92%, RF at 86%, SVM at 89%, LR at 890%, and DT at 73%. The specificity of a test is calculated using (9).

$$Specificity = \frac{TN}{TN + FP} \tag{9}$$

Table 4. Comparison of existing models with results of the proposed model using six performance measures

Model name	Model name Accuracy		Recall	F1-SCORE	AUC-ROC	Specificity	
	(%)	(%)	(%)	(%)	(%)	(%)	
DT [3]	80	82	78	80	88	73	
LR [5]	85	88	82	85	91	86	
SVM [7]	87	89	85	87	92	89	
RF [1]	88	90	86	88	93	90	
ANN [4]	89	92	88	90	94	92	
DenseNet-121 [Proposed model]	96.12	93.2	90	91	94.5	94	

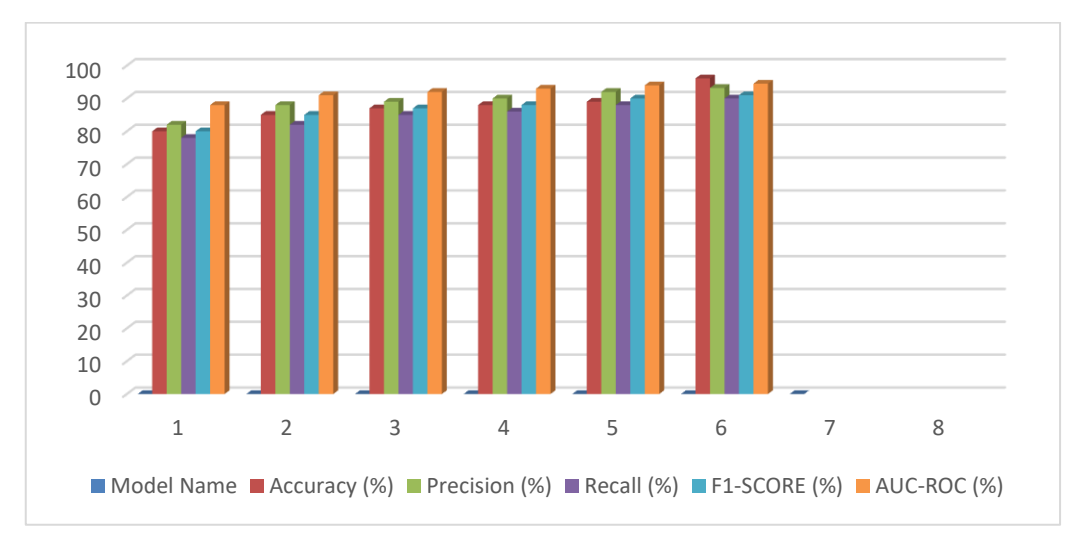


Figure 10. Comparison of performance measures with various models graphically

4.1. Key findings

The results of this research emphasize the superior performance of the proposed DenseNet-121 model in detecting the MPV. Specifically, we found that the DenseNet-121 model achieved significantly higher accuracy (96.12%) and precision (93.2%) compared to other models such as ANN, RF, and SVM. This model also demonstrated a strong recall (90%) and an impressive AUC-ROC (94.5%), indicating its robust predictive capabilities. Notably, the high specificity (94%) achieved by DenseNet-121 shows its efficiency in minimizing false positives, which is crucial in clinical settings.

Compared to models evaluated in other studies, the higher precision and recall of DenseNet-121 suggest that it is particularly effective in balancing sensitivity and specificity in detecting monkeypox. For instance, prior research by Rabie and Saleh [11] indicated that while high recall often leads to more false positives in ensemble classification methods, the findings suggest that DenseNet-121 mitigates this issue,

450 ☐ ISSN: 2252-8814

achieving high recall without compromising specificity. Additionally, unlike models like SVM and RF, which struggle with imbalanced datasets, comparative reviews found that AI methods like LSTM neural networks had limited accuracy (81.3%) in such conditions [10]. In contrast, the DenseNet-121 model in this paper maintains high accuracy and F1-score, offering improved performance [24]. These results also align with findings from Azar *et al.* [17], where DNNs showed success in image-based medical diagnostics. However, the DenseNet-121 model's dense block structure and data augmentation techniques provide an edge in the monkeypox detection context. However, this research extends these findings by applying extensive data augmentation techniques that further enhance generalization and performance [25].

While the results demonstrate that DenseNet-121 outperforms other models, this paper is not without limitations. The model's performance is strongly dependent on the quality and diversity of the training data [26]. Given the potential for biased or insufficient datasets, the generalization of this model may be affected in settings with different types of image data [27]. Moreover, the high computational requirements of DenseNet-121 limit its feasibility in resource-constrained environments. Further research is necessary to explore the model's performance with more extensive and varied datasets and to assess its real-world applicability in diverse clinical settings [28]. This paper paves the way for future exploration of DL models in disease diagnostics. The research shows that DenseNet-121 is more resilient to overfitting due to the use of extensive data augmentation, suggesting that future research may focus on even more advanced augmentation techniques or hybrid models. Additionally, there is potential to integrate clinical data with image-based diagnostics to improve diagnostic accuracy further [29]. Future studies could also explore transfer learning from other pre-trained models to detect similar infectious diseases, expanding the model's application beyond monkeypox detection.

5. CONCLUSION

The proposed DenseNet-121 model stands as a benchmark for the detection of the MPV, demonstrating exceptional efficacy across various performance metrics. One of the most significant merits of DenseNet-121 is its high recall (sensitivity) of 90%, which ensures a low false negative rate, crucial for the early detection and timely intervention of monkeypox cases. The model's accuracy of 96.12% and low FPR further affirm its reliability, ensuring that detected cases are indeed instances of monkeypox. Additionally, the model boasts a high F1-score of 91% and an impressive AUC-ROC of 94.5%, highlighting its robust performance and predictive capability. DenseNet-121 offers several key advantages. Its high sensitivity of 90% and accuracy of 96.12% ensure reliable detection of monkeypox cases, minimizing both false negatives and false positives. The model's robustness is further highlighted by its high F1-score of 91% and AUC-ROC of 94.5%, indicating its strong predictive capability. Additionally, the effective use of data augmentation techniques enhances the model's generalization capabilities, making it a reliable tool for diverse image data. Despite its strengths, the DenseNet-121 model has limitations. Its performance is heavily dependent on the quality and diversity of the training data, with limited or biased data potentially affecting its generalization ability. Moreover, training and deploying DenseNet-121 require significant computational resources, which might be a constraint in resource-limited settings. There is also a risk of overfitting, necessitating continuous monitoring and regular updates with new data to maintain its effectiveness. Overall, this paper provides definitive proof of the DenseNet-121 model's superior performance in detecting monkeypox, achieving higher accuracy, precision, and recall compared to other models. The high specificity (94%) and AUC-ROC (94.5%) underscore its robustness, minimizing both false negatives and false positives. The findings confirm that the model's performance is linked to its architecture and effective use of data augmentation rather than the volume of data alone. The novelty of the proposed model lies in its application of the DenseNet-121 architecture to the specific task of monkeypox detection, combined with extensive data augmentation techniques to enhance performance. By leveraging pre-trained networks on ImageNet and fine-tuning them for the unique challenges presented by monkeypox image data, the model not only ensures high accuracy but also significantly reduces the training time and processing efforts in contrast to training a model from scratch. While the DenseNet-121 model demonstrates outstanding potential for monkeypox detection, its dependency on data quality and computational resources highlights the need for continued research in optimizing these models for broader clinical applications. Overall, this model represents a significant advancement in infectious disease diagnostics, and future research can focus on refining these methods to address other similar health challenges. Applying more pragmatic data augmentation techniques can improve the model's generalization. The application of transfer learning from other pre-trained models might enhance detection capabilities. Integrating image-based diagnostics with clinical data can improve the overall diagnostic accuracy and reliability. Developing and testing the model in real-time clinical settings will assess its practical applicability and performance. Additionally, extending the model to detect other similar infectious diseases can broaden its scope and utility in medical diagnostics. The DenseNet-121 model proves to be a leading solution for the early, accurate, and reliable detection of monkeypox. Its outstanding performance across various metrics underscores its potential in advancing infectious disease diagnostics, with future research poised to enhance further and expand its capabilities.

FUNDING INFORMATION

Authors state no funding involved.

AUTHOR CONTRIBUTIONS STATEMENT

This journal uses the Contributor Roles Taxonomy (CRediT) to recognize individual author contributions, reduce authorship disputes, and facilitate collaboration.

Name of Author	C	M	So	Va	Fo	I	R	D	0	E	Vi	Su	P	Fu
Kishor Kumar Reddy	\checkmark	✓			✓	✓	✓		✓					
Chinthala														
Vijaya Sindhoori Kaza		\checkmark			\checkmark	\checkmark		\checkmark	✓	\checkmark				
Pilly Ashritha	✓				\checkmark		✓		✓					
Mohammed Shuaib	✓	✓				\checkmark		\checkmark	✓	\checkmark				
Shadab Alam		\checkmark			\checkmark		✓		✓	✓				
Mohammad Fakhreldin		\checkmark			✓			\checkmark	✓	\checkmark				

Fo: **Fo**rmal analysis E: Writing - Review & **E**diting

CONFLICT OF INTEREST STATEMENT

Authors state no conflict of interest.

DATA AVAILABILITY

The authors confirm that the data supporting the findings of this study are available within the article.

REFERENCES

- [1] M. Curaudeau, C. Besombes, E. Nakouné, A. Fontanet, A. Gessain, and A. Hassanin, "Identifying the most probable mammal reservoir hosts for monkeypox virus based on ecological niche comparisons," *Viruses*, vol. 15, no. 3, 2023, doi: 10.3390/v15030727.
- [2] K. N. Durski, "Emergence of monkeypox in West Africa and Central Africa, 1970–2017," Releve epidemiologique hebdomadaire, vol. 93, no. 11, pp. 125–132, 2018.
- [3] J. Ferdous, M. A. Barek, M. S. Hossen, K. K. Bhowmik, and M. S. Islam, "A review on monkeypox virus outbreak: new challenge for world," *Health Science Reports*, vol. 6, no. 1, 2023, doi: 10.1002/hsr2.1007.
- [4] I. Arita, Z. Jezek, L. Khodakevich, and K. Ruti, "Human monkeypox: a newly emerged orthopoxvirus zoonosis in the tropical rain forests of Africa," *American Journal of Tropical Medicine and Hygiene*, vol. 34, no. 4, pp. 781–789, 1985, doi: 10.4269/ajtmh.1985.34.781.
- [5] V. Singh, S. A. Khan, S. K. Yadav, and Y. Akhter, "Modeling global monkeypox infection spread data: a comparative study of time series regression and machine learning models," *Current Microbiology*, vol. 81, no. 1, 2024, doi: 10.1007/s00284-023-03531-6.
- [6] CDC, "Mpox in the United States and around the world: current situation summary," CDC, 2022. (accessed Jan. 31, 2025), [Online]. Available: https://www.cdc.gov/poxvirus/mpox/index.html.
- [7] Y. Li et al., "Evaluation of stability, inactivation, and disinfection effectiveness of Mpox virus," Viruses, vol. 16, no. 1, 2024, doi: 10.3390/v16010104.
- [8] C. Vazquez et al., "Exploring the genomic dynamics of the monkeypox epidemic in Paraguay," Viruses, vol. 16, no. 1, 2024, doi: 10.3390/v16010083.
- [9] S. L. Haller, C. Peng, G. McFadden, and S. Rothenburg, "Poxviruses and the evolution of host range and virulence," *Infection, Genetics and Evolution*, vol. 21, pp. 15–40, 2014, doi: 10.1016/j.meegid.2013.10.014.
- [10] X. Huang et al., "Loop-mediated isothermal amplification combined with lateral flow biosensor for rapid and sensitive detection of monkeypox virus," Frontiers in Public Health, vol. 11, 2023, doi: 10.3389/fpubh.2023.1132896.
- [11] A. H. Rabie and A. I. Saleh, "Monkeypox diagnosis using ensemble classification," *Artificial Intelligence in Medicine*, vol. 143, 2023, doi: 10.1016/j.artmed.2023.102618.
- [12] N. K. Sheeja, S. M. K, and S. Cherukodan, "Growth and dimensions of monkeypox research: a scientometrics study," Global Knowledge, Memory and Communication, 2023, doi: 10.1108/GKMC-04-2023-0120.

[13] L. Vierbaum et al., "Results of the first German external quality assessment scheme for the detection of monkeypox virus DNA," PLoS ONE, vol. 18, no. 4 April, 2023, doi: 10.1371/journal.pone.0285203.

- [14] T. Y. Taha et al., "Design and optimization of a monkeypox virus specific serological assay," Pathogens, vol. 12, no. 3, 2023, doi: 10.3390/pathogens12030396.
- [15] A. S. Jaradat et al., "Automated monkeypox skin lesion detection using deep learning and transfer learning techniques," International Journal of Environmental Research and Public Health, vol. 20, no. 5, 2023, doi: 10.3390/ijerph20054422.
- [16] I. Priyadarshini, P. Mohanty, R. Kumar, and D. Taniar, "Monkeypox outbreak analysis: an extensive study using machine learning models and time series analysis," *Computers*, vol. 12, no. 2, 2023, doi: 10.3390/computers12020036.
- [17] A. S. Azar, A. Naemi, S. B. Rikan, J. B. Mohasefi, H. Pirnejad, and U. K. Wiil, "Monkeypox detection using deep neural networks," BMC Infectious Diseases, vol. 23, no. 1, 2023, doi: 10.1186/s12879-023-08408-4.
- [18] P. R. Anisha, C. K. K. Reddy, M. M. Hanafiah, B. R. Murthy, R. M. Mohana, and Y. V. S. S. Pragathi, "An intelligent deep feature based metabolism syndrome prediction system for sleep disorder diseases," *Multimedia Tools and Applications*, vol. 83, no. 17, pp. 51267–51290, 2024, doi: 10.1007/s11042-023-17296-4.
- [19] C. K. K. Reddy et al., "A fine-tuned vision transformer based enhanced multi-class brain tumor classification using MRI scan imagery," Frontiers in Oncology, vol. 14, 2024, doi: 10.3389/fonc.2024.1400341.
- [20] K. K. Reddy C, A. Rangarajan, D. Rangarajan, M. Shuaib, F. Jeribi, and S. Alam, "A transfer learning approach: early prediction of Alzheimer's disease on us healthy aging dataset," *Mathematics*, vol. 12, no. 14, 2024, doi: 10.3390/math12142204.
- [21] K. K. R. Chinthala, M. S. Thakur, M. Shuaib, and S. Alam, "Prospects of computational intelligence in society: human-centric solutions, challenges, and research areas," *Journal of Computational and Cognitive Engineering*, vol. 00, no. September, pp. 1–14, 2024, doi: 10.47852/bonviewJCCE42023330.
- [22] A. Singh, K. Joshi, S. Alam, S. Bharany, M. Shuaib, and S. Ahmad, "Internet of things-based integrated remote electronic health surveillance and alert system: a review," 2022 IEEE International Conference on Current Development in Engineering and Technology (CCET), 2022, doi: 10.1109/CCET56606.2022.10080629.
- [23] M. Grossegesse *et al.*, "Serological methods for the detection of antibodies against monkeypox virus applicable for laboratories with different biosafety levels," *Journal of Medical Virology*, vol. 95, no. 12, 2023, doi: 10.1002/jmv.29261.
- [24] B. Long, F. Tan, and M. Newman, "Forecasting the monkeypox outbreak using ARIMA, prophet, neural prophet, and LSTM models in the United States," *Forecasting*, vol. 5, no. 1, pp. 127–137, 2023, doi: 10.3390/forecast5010005.
- [25] A. Khan, S. Zubair, M. Shuaib, A. Sheneamer, S. Alam, and B. Assiri, "Development of a robust parallel and multi-composite machine learning model for improved diagnosis of Alzheimer's disease: correlation with dementia-associated drug usage and AT(N) protein biomarkers," *Frontiers in Neuroscience*, vol. 18, 2024, doi: 10.3389/fnins.2024.1391465.
- [26] M. M. Ahsan et al., "Monkeypox diagnosis with interpretable deep learning," IEEE Access, vol. 11, pp. 81965–81980, 2023, doi: 10.1109/ACCESS.2023.3300793.
- [27] A. Farzipour, R. Elmi, and H. Nasiri, "Detection of monkeypox cases based on symptoms using XGboost and Shapley additive explanations methods," *Diagnostics*, vol. 13, no. 14, 2023, doi: 10.3390/diagnostics13142391.
- [28] K. Arora, M. Saxena, A. K. Sahoo, A. Maurya, P. K. Sarangi, and M. Dutta, "Using deep learning algorithms for accurate diagnosis and outbreak prediction of monkeypox," 4th International Conference on Innovative Practices in Technology and Management 2024, ICIPTM 2024, 2024, doi: 10.1109/ICIPTM59628.2024.10563418.
- [29] L. Alnaji, "Machine learning in epidemiology: neural networks forecasting of monkeypox cases," *PLoS ONE*, vol. 19, no. 5, 2024, doi: 10.1371/journal.pone.0300216.

BIOGRAPHIES OF AUTHORS





Vijaya Sindhoori Kaza is a systems software engineer at Hewlett Packard Enterprise (HPE) in the HPC and AI division. She pursued her bachelor's in Computer Science at Stanley College of Engineering and completed her degree in 2024. She has been actively involved as a research assistant, contributing to and publishing several research papers in prestigious national and international conferences, book chapters, and journals indexed by Scopus and SCIE. She has also gained valuable work experience by completing internships at renowned companies like VMware and government organizations like DRDO. She is also collaborating and co-authoring research papers with professors from various reputed institutions. Her research interests span across artificial intelligence, machine learning, deep learning, cognitive science, genomics, and bioinformatics. She is passionate about exploring the interdisciplinary aspects of these fields to develop innovative solutions and advance the understanding of computational methods and AI in bioinformatics. She aspires to make impactful research contributions in the field of AI and its applications in bioinformatics. She can be contacted at email: vijaya.sindhoori@gmail.com.



Pilly Ashritha is a B.E. graduate from the Department of Computer Science and Engineering at Stanley College of Engineering and Technology for Women in Hyderabad, India. With two years of research experience, she has participated in international internships and possesses extensive knowledge of global research trends. Ashritha has authored three book chapters and co-authored over four additional chapters and journals. Her research interests encompass weather forecasting, natural disasters, the effects of artificial intelligence, and digital transformation. She can be contacted at email: ashrithapilly22@gmail.com.



Mohammed Shuaib D S completed his Master of Technology in Computer Engineering at Aligarh Muslim University, India. He later earned his PhD in Computer Engineering from the Razak Faculty of Technology and Informatics at Universiti Teknologi Malaysia, Malaysia. Currently, Mohammed Shuaib is working in the Department of Computer Science and Engineering at Jazan University, K.S.A. He holds a position as a Visiting Research Fellow at the Faculty of Information Technology, INTI International University, Malaysia. His research interests include self-sovereign identity, blockchain, information security, IoT, identity management, cloud computing, cyber-physical systems, and sensor networks. Mohammed Shuaib has authored 21 scientific articles published in internationally recognized journals, including Elsevier, IEEE, and Springer, all indexed by the Web of Science. He holds four patents in his field and has contributed to numerous educational workshops and seminars. His research extends to various editorial responsibilities, serving as an Associate Editor for Sustainable Computing at Elsevier, Academic Editor for PLOS ONE, and an Editorial board member for Discover Internet of Things at Springer and Frontiers in Blockchain. He is actively involved with several editorial boards, including the Journal of Economy and Technology at Elsevier and the International Journal of Advances in Applied Sciences by IAES. He can be contacted through email: talkshuaib@gmail.com.



Shadab Alam is surrently working as an Associate Professor in the Department of Computer Science at Jazan University, Jazan, KSA, and holds a position as a Visiting Research Fellow at the Faculty of Information Technology, INTI International University, Malaysia. He earned a doctoral degree in Computer Science from Aligarh Muslim University, Aligarh, as well as a bachelor's and master's degree in computer science. His main areas of research are cryptography and information security, and his further research interests include the Internet of Things (IoT), Blockchain technology, and smart healthcare. He has published more than 80 research papers in reputed journals and international conference proceedings. He holds seven patents in his domain and is working as an editor for several reputed journals like PLOS One, SUSCOM, etc. He is a senior member of IEEE (SMIEEE) and a member of CSI, CRSI, ACM, IAENG, CSTA, IACSIT, and ICSE. He can be contacted through email: snafis@jazanu.edu.sa.



Mohammad Fakhreldin is an Assistant Professor at the Faculty of Computer Science and Information Technology, College of Engineering and Computer Science, Jazan University, Saudi Arabia. His research interests include machine learning and image processing. He can be contacted through email: mfakhreldin@jazanu.edu.sa.